Atmos. Meas. Tech., 5, 1387–1398, 2012
www.atmos-meas-tech.net/5/1387/2012/
doi:10.5194/amt-5-1387-2012

Atmospheric Measurement Techniques

CH_4, CO, and H_2O spectroscopy for the Sentinel-5 Precursor mission: an assessment with the Total Carbon Column Observing Network measurements

A. Galli[1], A. Butz[2], R. A. Scheepmaker[1], O. Hasekamp[1], J. Landgraf[1], P. Tol[1], D. Wunch[3], N. M. Deutscher[4,5], G. C. Toon[6], P. O. Wennberg[3], D. W. T. Griffith[4], and I. Aben[1]

[1]Netherlands Institute for Space Research (SRON), 3584 CA Utrecht, The Netherlands
[2]Karlsruhe Institute of Technology, Institute for Meteorology and Climate Research, 76344 Leopoldshafen, Germany
[3]Department of Earth Science and Engineering, California Institute of Technology, Pasadena, CA 91125, USA
[4]Centre for Atmospheric Chemistry, University of Wollongong, Wollongong, NSW 2522, Australia
[5]Institute of Environmental Physics, University of Bremen, 28334 Bremen, Germany
[6]Jet Propulsion Laboratory, California Institute of Technology, Pasadena, CA 91125, USA

Correspondence to: A. Galli (a.galli@sron.nl)

Received: 2 March 2012 – Published in Atmos. Meas. Tech. Discuss.: 13 March 2012
Revised: 18 May 2012 – Accepted: 29 May 2012 – Published: 19 June 2012

Abstract. The TROPOspheric Monitoring Instrument (TROPOMI) will be part of ESA's Sentinel-5 Precursor (S5P) satellite platform scheduled for launch in 2015. TROPOMI will monitor methane and carbon monoxide concentrations in the Earth's atmosphere by measuring spectra of back-scattered sunlight in the short-wave infrared (SWIR).

S5P will be the first satellite mission to rely uniquely on the spectral window at 4190–4340 cm^{-1} (2.3 µm) to retrieve CH_4 and CO. In this study, we investigated if the absorption features of the three relevant molecules CH_4, CO, and H_2O are adequately known. To this end, we retrieved total columns of CH_4, CO, and H_2O from absorption spectra measured by two ground-based Fourier transform spectrometers that are part of the Total Carbon Column Observing Network (TCCON). The retrieval results from the 4190–4340 cm^{-1} range at the TROPOMI resolution (0.45 cm^{-1}) were then compared to the CH_4 results obtained from the 6000 cm^{-1} region, and the CO results obtained from the 4190–4340 cm^{-1} region at the higher TCCON resolution (0.02 cm^{-1}).

For TROPOMI-like settings, we were able to reproduce the CH_4 columns to an accuracy of 0.3 % apart from a constant bias of 1 %. The CO retrieval accuracy was, through interference, systematically influenced by the shortcomings of the CH_4 and H_2O spectroscopy. In contrast to CH_4, the CO column error also varied significantly with atmospheric H_2O content. Unaddressed, this would introduce seasonal and latitudinal biases to the CO columns retrieved from TROPOMI measurements. We therefore recommend further effort from the spectroscopic community to be directed at the H_2O and CH_4 spectroscopy in the 4190–4340 cm^{-1} region.

1 Introduction

Methane (CH_4) and carbon monoxide (CO) have a large impact on climate variability and air quality. Accurate monitoring with high spatial and temporal coverage allows the scientific community to better model atmospheric chemistry, atmospheric transport, and land-atmosphere interactions (bush-fires, regional CH_4 emissions of wetlands and livestock, etc.). Both ground-based observations and satellite observations are currently used to monitor CH_4 and CO.

The Total Carbon Column Observing Network (TCCON) is a global network of ground-based Fourier transform spectrometers, established in 2004 (Wunch et al., 2011a). Its goal is to remotely measure column abundances of CO_2, CO, CH_4, N_2O and other molecules that absorb in the short-wave infrared (SWIR) and near-infrared (4000–15 000 cm^{-1}).

Currently, there are 18 operational observation sites affiliated with TCCON. TCCON measurements are used to validate satellite measurements (Butz et al., 2011; Morino et al., 2011; Parker et al., 2011; Wunch et al., 2011b; Reuter et al., 2011) and they also provide direct constraints on global greenhouse gas inventories (e.g. Yang et al., 2007; Fraser et al., 2011). Thanks to their high spectral resolution ($0.02\,cm^{-1}$), the measured spectra can also be used to evaluate spectroscopic databases (e.g. Tran et al., 2010).

ESA's Sentinel-5 Precursor (S5P) satellite – due for launch in early 2015 – will complement a series of polar-orbiting satellites that monitor CH_4 and CO concentrations in the Earth's atmosphere. Its payload, the TROPOspheric Monitoring Instrument (TROPOMI) (Veefkind, 2012), is an imaging spectrometer that will measure back-scattered solar radiation spectra in the nadir and off-nadir directions. TROPOMI will feature a wide swath of 2600 km with a ground pixel area of $7 \times 7\,km^2$ (for the sub-satellite point), which implies daily global coverage of the Earth's surface, with $\sim 7 \times 10^6$ measured spectra. The spectrometer will measure the SWIR range at 4190–4340 cm^{-1} with moderate spectral resolution ($0.45\,cm^{-1}$). This range covers strong absorption lines by CH_4 and water vapour (H_2O) as well as weak absorption by CO and deuterated water (HDO).

During one decade of operations, the SCanning Imaging Absorption spectroMeter for Atmospheric CartograpHY (SCIAMACHY) (Bovensmann et al., 1999) has demonstrated that this type of satellite observation allows for the retrieval of total atmospheric columns of CH_4 (e.g. Frankenberg et al., 2006; Bergamaschi et al., 2009) and CO (Buchwitz et al., 2007; de Laat et al., 2010). Since February 2009, the Greenhouse gases Observing SATellite (GOSAT) (Kuze et al., 2009) is providing CO_2 and CH_4 concentration measurements as well, which are currently subject to validation (Butz et al., 2011; Morino et al., 2011; Wunch et al., 2010; Parker et al., 2011). A satellite observation set of tropospheric CO is provided by the Measurements Of Pollution In The Troposphere (MOPITT) instrument, active since the year 2000. CO total columns and vertical profiles both from the SWIR and from the thermal-infrared near $2100\,cm^{-1}$ are retrieved from the MOPITT data (Deeter et al., 2009). In the coming years, S5P will fill the gap between the currently orbiting satellites and later missions such as Sentinel-5. A common goal of these missions is to monitor atmospheric CH_4 concentrations with the accuracy and spatio-temporal coverage that enable inverse modelling of CH_4 sources on regional and weekly scales. S5P will also provide users with a CO product at high spatial and temporal sampling, a single measurement having an uncertainty of 10 % at most. In contrast, SCIAMACHY data have to be averaged in time (roughly one month) and space ($\sim 5^\circ \times 5^\circ$) to reach a comparable accuracy.

The absorption lines of CH_4 and CO in the SWIR can be used to infer the total atmospheric concentration with high sensitivity to the Earth's surface and lower atmosphere where sources are located. Measurements in the thermal-infared are usually less sensitive to CO in the lower troposphere. The main challenge for the inversion technique is the desired accuracy: for CH_4, residual retrieval biases as small as $\sim$0.4 % could be detrimental to inverse modelling of sources and sinks (Bergamaschi et al., 2009). The scientific objective for CO – an overall accuracy of better than 15 % (Vidot et al., 2012) – seems less demanding, but the CO absorption lines are hard to detect among the strong absorption lines of CH_4 and H_2O. The retrieval accuracy depends on accurate knowledge of the light path of the back-scattered sunlight through the Earth's atmosphere. Scattering by particles such as aerosols, water and cirrus clouds can modify the light path and induce retrieval errors. The two studies published recently by Butz et al. (2012) and Vidot et al. (2012) focused on this error source and – using synthetic input spectra – concluded that the scientific goals of TROPOMI can be achieved with the predicted instrumentation. Butz et al. (2012) cautioned, however, that a few other, unrelated, error sources had not yet been assessed. One of them, which is hard to assess by means of synthetic input spectra alone, is the inaccuracy of the assumed molecular absorption lines of CH_4, CO, and H_2O. This error source is the topic of this study. It is representative for the spectroscopy-related errors in TROPOMI retrievals with a low density of scatterers in the forward model.

To assess these errors, we will retrieve CH_4 and CO columns from the spectra of ground-based Fourier transform spectrometers at two different locations, both at their native high resolution ($0.02\,cm^{-1}$) and convolved with the TROPOMI instrument response function to produce lower-resolution spectra ($0.45\,cm^{-1}$). The results of the retrievals in the 4190–4340 cm^{-1} range will then be compared to the reference values obtained from 5880–6174 cm^{-1} (for CH_4), and from 4209–4313 cm^{-1} (for CO) at the native resolution. The paper is structured in the following way: in Sect. 2, we will characterise the measurements and the inversion method to evaluate them. The results and their implications for the spectroscopic databases of CH_4, H_2O, and CO will be presented in Sect. 3. Section 4 will conclude the paper with recommendations for the S5P mission.

2 Methodology

In this section, we present the TCCON observations and the different spectral ranges used for this study (Sect. 2.1), before explaining our forward model (Sect. 2.2) and the inversion method (Sect. 2.3). After verification of our inverse method (in Sect. 2.4) the approach to analyse the results is described in Sect. 2.5.

2.1 TCCON observations

We chose two sets of TCCON observations to cover both wet and dry atmospheric conditions: 50 spectra measured at Darwin (in the tropical Northern region of Australia) between December 2005 and November 2007, and 50 spectra measured at Park Falls (inland, close to the US-Canadian border) between July 2004 and February 2006 (Deutscher et al., 2010; Washenfelder et al., 2006). Each of the 100 spectra was measured on a different day, the days being evenly distributed in time. The Park Falls data cover a large range of solar zenith angles (SZA) between 20 and 80 degrees. The Darwin spectra have a narrower spread in observation geometry ($35 < \mathrm{SZA} < 45$ degrees for 48 of 50 spectra). For evaluation, we split the spectra into the ranges listed in Table 1 and, whenever TROPOMI spectra were to be simulated, convolved them with the expected TROPOMI instrument response function (Sect. 2.2).

Table 1 summarises all spectral windows referred to in this study. The windows used for GFIT are windows 1, 2, and 3 for CH_4, the windows labelled 4 for H_2O, and the windows labelled 5 for CO. Windows 6a and 6b cover the expected spectral range for TROPOMI. The original resolution corresponds to a full width half maximum (FWHM) of $0.0134\,\mathrm{cm}^{-1}$ (window 6a), and the TROPOMI resolution has a a FWHM of $0.45\,\mathrm{cm}^{-1}$ (window 6b).

Table 1. Overview of spectral ranges used for inversion.

window number	wave number range (cm^{-1})	target species	other absorbers
1	5880–5996	CH_4	CO_2, H_2O
2	5996.45–6007.55	CH_4	CO_2, H_2O
3	6007–6145	CH_4	CO_2, H_2O
4	6073.05–6080.75, 6098.4–6100.3, 6124.4–6127.3, 6176.47–6178.13, 6252.35–6259.55, 6293.45–6309.25, 6389.35–6395.55, 6400.0–6402.3, 6466.1–6473.1	H_2O	CH_4, CO_2
5	4208.7–4257.3, 4262–4318.8	CO	H_2O, HDO, CH_4
6a	4190–4340 TCCON resolution	CH_4, CO	H_2O, HDO
6b	4190–4340 TROPOMI resolution	CH_4, CO	H_2O, HDO

2.2 Forward model

In contrast to the more elaborate forward model required to invert back-scattered sunlight spectra (Hasekamp and Butz, 2008), the forward model in this study neglects scattering processes. The TCCON spectrometers measure direct sunlight, which is, to a good approximation, only affected by molecular absorption on its way through the atmosphere (Wunch et al., 2011a). The modelled signal $\boldsymbol{F}(k)$ can be written as an integral over the entire height h of the atmosphere

$$\boldsymbol{F}(k) = \mathbf{R} \otimes \boldsymbol{S}_{\odot}\, g \exp\left(-\int_0^{\infty} \mathrm{d}h\, n(h)\, \sigma\,(p, T, k)\; f\,(\mu_0)\right). \quad (1)$$

$\boldsymbol{S}_{\odot}$ denotes the solar radiance, for which we adopted the solar line list used by the TCCON science team (G. C. Toon, private communication, 2010). The other terms in Eq. (1) are the instrument gain g, the wave number of the spectrum k, the pressure and temperature p and T, the molecular cross-sections $\sigma\,(p, T, k)$, the particle density of the considered absorber molecules $n(h)$, and finally $f\,(\mu_0)$, the airmass as a function of $\mu_0 = \cos(\mathrm{SZA})$ (Kasten and Young, 1989). After integrating over height and atmospheric constituents, one needs to convolve the modelled absorption spectrum with the instrument response function $\mathbf{R}$ before comparing it to the measurements. To reproduce the TCCON retrieval values, we assumed the instrument line shape to be a sinc function convolved with a rectangular function, with $0.02\,\mathrm{cm}^{-1}$ between the first zero-crossings (corresponding to $\mathrm{FWHM} = 0.0134\,\mathrm{cm}^{-1}$) and an oversampling rate of $1.9 \times \mathrm{FWHM}$. To simulate TROPOMI-like spectra, we convolved the TCCON spectra with a Gaussian instrument line shape with a coarser FWHM of $0.45\,\mathrm{cm}^{-1}$ and an oversampling rate of $2.5 \times \mathrm{FWHM}$. Figure 1 shows the two spectral resolutions in the SWIR window between 4190 and $4340\,\mathrm{cm}^{-1}$.

The HITRAN 2008 molecular spectroscopic database (HITRAN08, Rothman et al., 2009) served as our default cross-section database, with the exception of the H_2O line lists. For H_2O in windows 1 to 4, we combined the line list by Jenouvrier et al. (2007) with HITRAN08 by selecting for each absorption line the version that produced the smaller spectral fit residuals. For the TROPOMI range at 4190–$4340\,\mathrm{cm}^{-1}$, we used the line list developed by Scheepmaker et al. (2012). These line lists are not identical to the H_2O spectroscopy used by the TCCON science team. The latter improved the fit quality in spectral window 1, whereas it led to larger fit residuals in the TROPOMI range. To keep the paper short, we will only present retrievals obtained with the H_2O line lists developed for this study. The CH_4, CO, and CO_2 line lists used in the GFIT algorithm are the HITRAN08 line lists that were also used for this study. Figure 2 shows the relative strength of the CH_4, H_2O, and CO absorption features in the range of 4190–4340 cm^{-1}. The cross-sections were evaluated at $p = 1000\,\mathrm{hPa}$, $T = 296\,\mathrm{K}$ and multiplied with columns

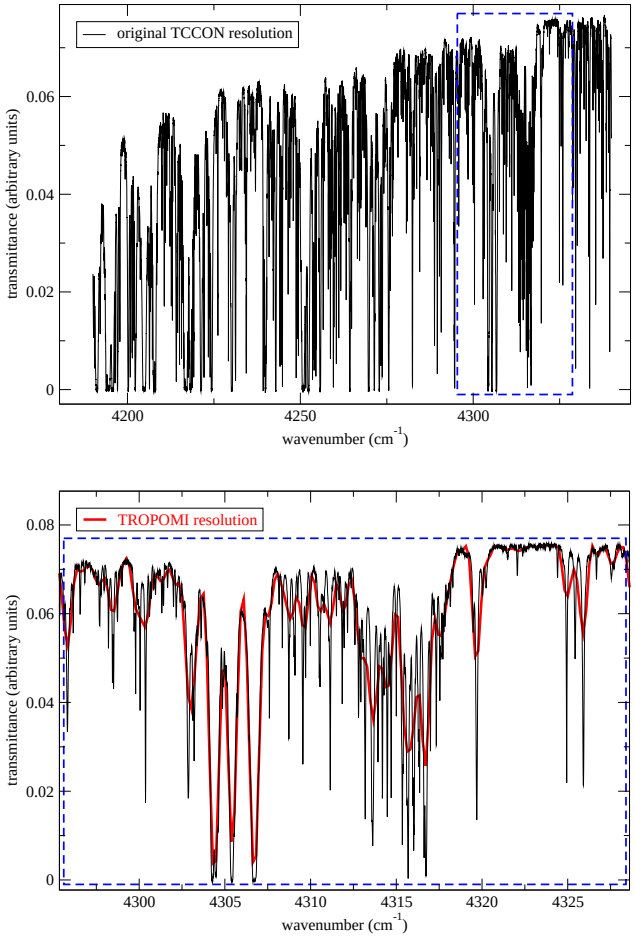

Fig. 1. Upper panel: original TCCON spectrum of the TROPOMI wave number range 4190–4340 cm^{-1}, measured at Darwin. Lower panel: magnification of the 4300–4325 cm^{-1} range (blue dashed box) with both the original spectrum (black) and the same spectrum, convolved with the TROPOMI instrument response function (red).

N_i representative for observations at Darwin to obtain approximate optical depths (Eq. 1).

2.3 Inverse method

We used the same inversion approach as described by Butz et al. (2012). We optimised the state vector $\boldsymbol{x}$, subjected to the forward model $\boldsymbol{F}$ (Eq. 1), from the TCCON measurements $\boldsymbol{y}$ by minimising Eq. (2). The state vector $\boldsymbol{x}$ contained the following elements: total column number density $N_i = \sum n_i(h)$ for CO and H_2O, a profile for CH_4, three parameters to fit a wave number dependent instrumental gain g, and two auxiliary parameters to compensate for a spectral shift of the measured spectrum with respect to the tabulated cross-sections. By default, pressure, temperature, and the height profiles of the absorbing species were not retrieved in the state vector. We assumed a fixed a priori atmospheric profile for CH_4, H_2O, and CO, and fitted only a scalar correction factor to the

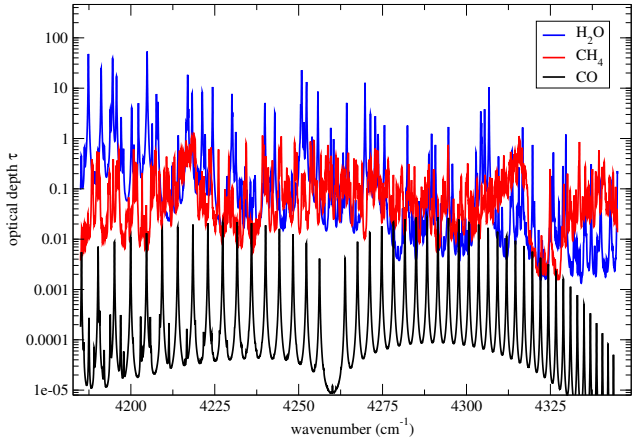

Fig. 2. Approximate optical depth versus wave numbers, attributed to the three species considered for the spectral range 4190–4340 cm^{-1}: CH_4 (red), H_2O (blue), and CO (black).

initial N_i. The exception to this rule was CH_4. The spectral fit residuals decreased by 10 % when the CH_4 column was retrieved as a 12-layer height profile. The state vector thus contained twelve instead of one entry for CH_4. They were summed up in the end to yield a total CH_4 column. As for all other species, the degrees of freedom of the inversion (between 1.8 and 1.9) were insufficient to retrieve a meaningful profile.

To retrieve $\boldsymbol{x}$, regularisation is required because the inverse problem is ill-posed, i.e. the measurements $\boldsymbol{y}$ contain insufficient information to retrieve all state vector elements independently. The Phillips-Tikhonov regularisation method (Phillips, 1962; Tikhonov, 1963) finds the optimised state vector $\hat{\boldsymbol{x}}$ by minimising a cost function that is the sum of the least-squares cost function and a side constraint weighted by the regularisation parameter $\gamma \geq 0$ according to

$$\hat{\boldsymbol{x}} = \arg\min_x \left(\|\mathbf{S}_y^{-1/2} \boldsymbol{F}(\boldsymbol{x}) - \boldsymbol{y}\|^2 + \gamma \|\mathbf{W}\boldsymbol{x}\|^2 \right). \quad (2)$$

$\mathbf{W}$ is the weighting matrix, and $\mathbf{S}_y$ is the diagonal measurement error covariance matrix containing the noise estimate. For $\mathbf{S}_y$ we assumed a signal-to-noise ratio of 1000 (Wunch et al., 2011a).

The set-up of the atmospheric input was not changed with respect to Butz et al. (2012): the atmosphere was divided into a grid of 72 planar atmospheric layers (equidistant steps in terms of pressure). By default, temperature, pressure, and height were kept constant. The initial values for pressure, temperature and the H_2O profile were taken from the ECMWF (European Centre for Medium-Range Weather Forecasts) ERA-Interim analysis, provided 6-hourly on a $1.5° \times 1.5°$ latitude × longitude grid. We checked that the surface pressure agreed within 0.1 % to the pressure measured at the TCCON stations. For the CH_4 and CO a priori profiles, we relied on the chemistry transport model (TM4) profiles (Meirink et al., 2006). The a priori were obtained

from a one-year average at the corresponding geolocation of the observation sites.

2.4 Reference retrievals

Throughout this paper we used the atmospheric total columns N_i (in molecules cm^{-2}) obtained from the spectral ranges 5880–6174 cm^{-1} (for CH_4) and from 4209–4319 cm^{-1} (for CO) as reference values. These spectral ranges are also used by the TCCON science team for their retrievals with the GFIT nonlinear least squares spectral fitting algorithm. GFIT is a profile scaling retrieval which fixes the a priori profile shape of the absorber, and scales the profile to produce a calculated spectrum that best matches the measured spectrum. The surface pressure is measured at each TCCON station with a barometer (Wunch et al., 2011a). Dedicated effort in the past years to improve CH_4 and H_2O spectroscopy in the 5880–6174 cm^{-1} range (Frankenberg et al., 2008; Tran et al., 2010; Jenouvrier et al., 2007) has enabled accurate retrieval of CH_4 columns from this spectral range. This has been confirmed by validation of GFIT retrievals with independent aircraft measurements. Similarly, the accuracy of retrieved CO columns from the 4209–4319 cm^{-1} spectral range by GFIT has also been confirmed by validation with aircraft measurements (Wunch et al., 2010).

Our inversion algorithm being not identical to GFIT, we first verified our algorithm. We checked if it reproduces the CH_4 and CO total columns derived with GFIT when the same spectral ranges and spectral resolution were used (see Table 1). A complication arose when inter-comparison of our CH_4 results from windows 1, 2, and 3 showed that the retrieval quality from window 1 (5880–5996 cm^{-1}) was unsatisfying. A closer inspection revealed that there were several strong H_2O absorption lines not well captured by our line list. We therefore decided to discard window 1 altogether and reproduce the GFIT values for CH_4 from the average of windows 2 and 3. For all observation windows, the spectrum measured at Park Falls on 21 June 2005 turned out to produce much larger spectral fit residuals than the average. The GFIT retrieval also assigns large error bars to the columns retrieved from this spectrum. This data point was therefore omitted from further analysis.

Comparing our retrieved CH_4 values from windows 2 and 3 to the GFIT values, we found a bias between the two datasets of 0.1 % for both Parkfalls and Darwin and standard deviations of 0.26 % and 0.18 % for Park Falls and Darwin, respectively. These differences are not larger than the average uncertainty of the CH_4 column retrieved with the GFIT algorithm. The latter is 0.28 % for the Park Falls time-series and 0.22 % for the Darwin time-series. For CO, we found biases of 1.6 % and −2.8 %, and standard deviations of 1.1 % and 1.8 % for Park Falls and Darwin, respectively. The small differences between our algorithm and GFIT can be explained by the differences in averaging kernels and a priori profiles for CH_4, CO, and H_2O (smoothing and interference errors), and the differences in the H_2O line list. Therefore, we considered our retrieved columns from the 5880–6174 cm^{-1} range (for CH_4) and from 4209–4319 cm^{-1} range (for CO) as reference values and the standard deviations between the algorithms as the associated error σ_{ref}.

2.5 Analysis of the results

To discuss the retrieval accuracy, we used the following four diagnostic quantities throughout this study. They quantify by how much the quality of the retrieved columns decreased when CH_4, CO, and H_2O columns were retrieved from 4190–4340^{-1} at the TROPOMI resolution compared to the reference results (spectral ranges listed in Table 1). For the standard deviation, the bias, and the correlation coefficient, we interpreted the columns of CH_4, CO, and H_2O retrieved at Park Falls or Darwin as a time-series and compared it to the time-series of the reference values:

1. The reduced fit residual χ^2/ν: the sum of the residuals between modelled and measured spectrum, divided by the degrees of freedom ν (number of spectral pixels minus the degrees of freedom of the fit):

$$\chi^2/\nu = \sum_{k=1}^{K} \left(\frac{y_{\mathrm{meas},k} - y_{\mathrm{mod},k}}{\sigma_k} \right)^2 / \nu. \quad (3)$$

   The fit residual χ^2 equals the least-squares part of the cost function in Eq. (2). In the results section, we will list the average $\langle \chi^2/\nu \rangle$ over all spectra.

2. The σ_N standard deviation of the differences between the retrieved columns at TROPOMI-like settings and the reference values. This number serves as an estimate of the accuracy of our results including systematic errors. In the tables, we will always compare it to the error σ_{ref} of the reference retrievals. If σ_N is not much larger than σ_{ref}, the differences between the two retrievals are statistically insignificant.

3. The bias b of the new retrieval values with respect to the reference values, calculated from the median of the relative differences.

4. The correlation coefficient ξ between the new retrieval values and the reference values.

3 Results

In this section, we compare the inversion results (CH_4 in Sect. 3.1, CO in Sect. 3.2) for the TROPOMI spectral range to the reference retrievals. An option to improve the CO retrieval accuracy is presented in Sect. 3.3.

Table 2. Fit diagnostics of the CH_4 column retrievals in the 4190–4340 cm^{-1} range, for the original (TCCON) and for the TROPOMI resolution.

	$\langle\chi^2/\nu\rangle$	σ_N	σ_{ref}	b	ξ
Darwin TROPOMI	43	0.24 %	0.18 %	0.010	0.93
Park Falls TROPOMI	32	0.28 %	0.26 %	0.009	0.97
Darwin TCCON	106	0.28 %	0.18 %	0.008	0.91
Park Falls TCCON	83	0.29 %	0.26 %	0.004	0.97

3.1 CH_4 retrieval accuracy

Figure 3 shows the time-series of CH_4 columns (upper panel) and the differences (lower panel) between the results from the TROPOMI range and the 5996–6147 cm^{-1} range. The Darwin observations are coloured red, the Park Falls observations are shown in blue. In the lower panel, solid lines belong to retrievals at TROPOMI resolution (window 6b in Table 1), dotted lines denote results from the original resolution (window 6a). The dashed lines illustrate the biases for window 6b. Table 2 lists the fit diagnostics. Those are from left to right: average spectral fit residuals ($\langle\chi^2/\nu\rangle$), standard deviation of the differences in columns (σ_N) versus the reference error σ_{ref} (see Sect. 2.4), bias b, and correlation coefficient ξ. Table 2 shows that the CH_4 columns were well reproduced for TROPOMI-like settings. The average scatter of retrieved columns increased only from 0.18 to 0.24 % at Darwin, and from 0.26 to 0.28 % at Park Falls. Neither the standard deviation nor the correlation changed significantly when the original spectral resolution was assumed. The difference between the values derived from TROPOMI-like settings and the reference values from spectral windows 2 and 3 was not significant except for the two outliers in summer 2005 at Park Falls (Fig. 3). The error bars assigned to these values by the GFIT algorithm are also three times larger than the average value. The positive bias of roughly 1 % at both sites thus is the only evidence for spectroscopy-related errors affecting the CH_4 columns. This bias increased for the lower spectral resolution, which is consistent with interference errors due to inaccurate CH_4 or H_2O spectroscopy. The spectral fit residuals increased from ∼30 at the 6000 cm^{-1} range to ∼100, but they cannot be directly related to a column error.

To see if H_2O interference errors could account for the 1 % bias, we investigated the dependence of the CH_4 retrieval errors on the H_2O abundance. Figure 8, upper panel, shows CH_4 retrieval errors against H_2O dry air mole fraction (DMF) at Darwin, the air-mass being between 1.2 and 1.4 for all observations. The dashed line is the linear regression (correlation coefficient = 0.22), the dotted lines show the 1-σ uncertainty level of the slope. The slope is not significantly larger than zero at a 2-σ level and it increases only from 0.9 to 1.1 % for the range of observed H_2O DMF. This may be enough to account for the increase of the bias for the lower spectral

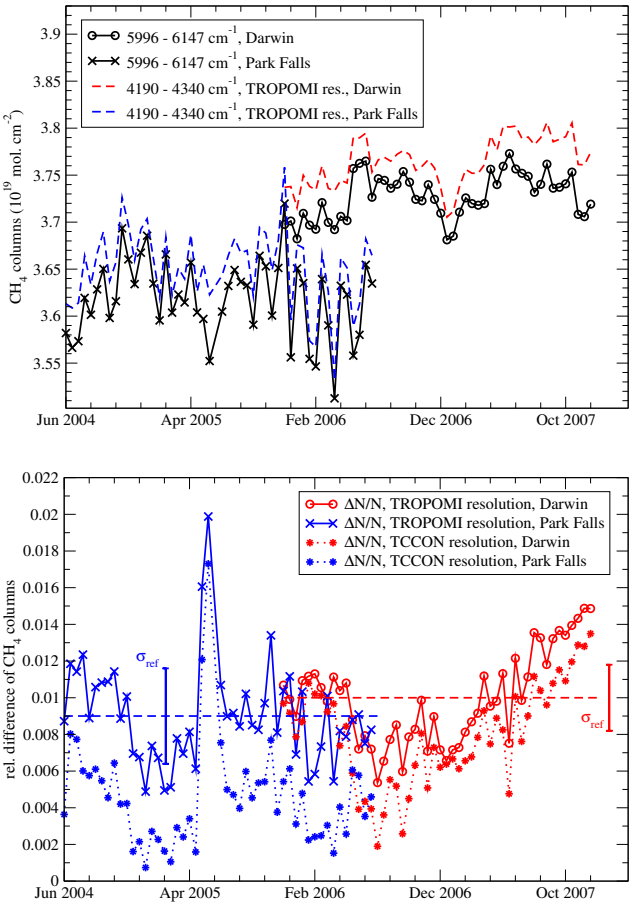

Fig. 3. CH_4 retrieval accuracy for the 4190–4340 cm^{-1} range. The upper panel shows the time-series of CH_4 columns at Park Falls (crosses) and at Darwin (circles). The lower panel shows the relative differences between columns retrieved at original (dotted lines) and at TROPOMI resolution (solid lines) with respect to reference values from 5996–6145 cm^{-1}.

resolution, but both effects are on the order of the reference retrieval accuracy.

Since there are no plans to retrieve O_2 from TROPOMI spectra, the surface pressure was treated as a fixed parameter in the inversion method up to this point. The TCCON spectra cover several strong O_2 absorption regions and can thus also be used to derive total O_2 columns and – if one assumes a constant atmospheric oxygen ratio – a surface pressure. To study the pressure-dependence of the spectroscopic line lists, we chose a different approach to avoid an assessment of O_2 spectroscopy. Instead of retrieving surface pressure and trace gas species separately, our inversion algorithm also allows for a simultaneous retrieval. For such a retrieval, the observation windows need not include O_2 absorption lines, since the line shape of any absorber depends on pressure. At each iteration step, then, the total dry air column is optimised with respect to the cross-sections of all retrieved molecules.

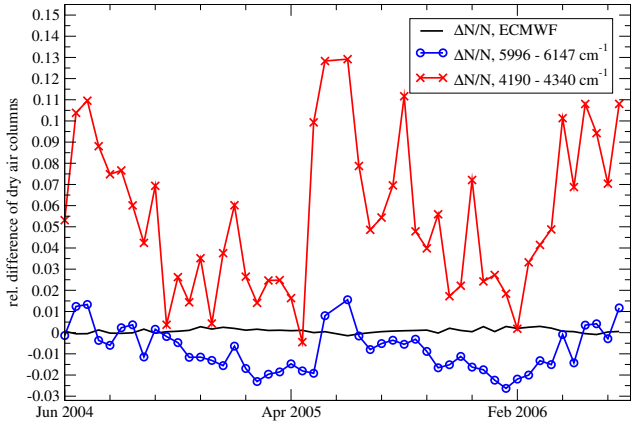

Fig. 4. Impact of spectroscopic line lists on derived pressure at Park Falls. Black: total dry air column for fixed ECMWF pressure profile, plotted as relative difference to in-situ measurement. Circles: dry air column derived from 5996–6145 cm^{-1}, crosses: dry air column derived from 4190–4340 cm^{-1}.

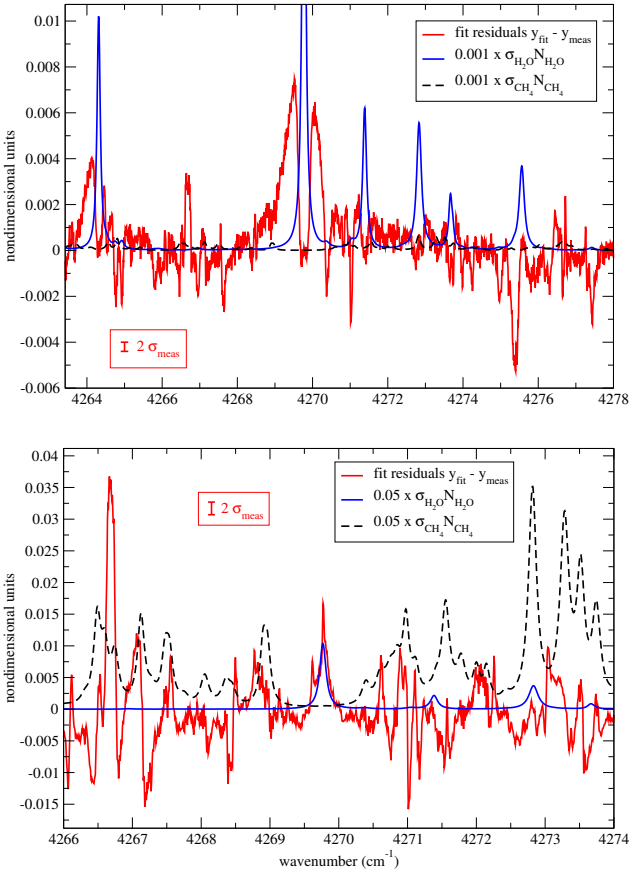

Fig. 5. Spectral fit residuals for wet atmospheric conditions at Darwin (upper panel) and for dry atmospheric conditions at Park Falls (lower panel). Fit residuals (red line) are over-plotted with optical depth of H_2O (blue line) and CH_4 (black dashed line), average measurement uncertainty indicated by error bars in boxes.

When we retrieved the surface pressure from the CH_4 and H_2O absorption features in the 5996–6145 cm^{-1} range, the dry air columns agreed with the in-situ measurements within 2 %. The same approach resulted in errors larger than 10 % when we chose the 4190–4340 cm^{-1} range. The difference in retrieved CH_4 columns were smaller (0.3 to 0.8 %), but still significant. Figure 4 shows the relative differences of retrieved dry air columns versus the value measured at the Park Falls site. Results from windows 2 and 3 (circles) are compared to the column errors from the TROPOMI spectral range (crosses). The dry air columns derived from the ECMWF pressure profile, which serve as our default, agree with the measured dry air columns within 0.1 % standard deviation (black curve in Fig. 4).

The failure to retrieve surface pressure from the SWIR band was probably caused by inaccurate pressure-broadening parameters of the CH_4 and H_2O line lists. As long as the pressure was kept fixed, these shortcomings manifested themselves primarily in the spectral fit residuals (see Fig. 5). If, however, the surface pressure was treated as a free parameter, the inversion routine optimised for a pressure which compensated for inaccurately predicted absorption line shapes. This resulted in values as far as 10 % away from the true surface pressure (see Fig. 4). CH_4 and H_2O were found to yield a comparable pressure over-estimation when only one of them was retrieved. The only region exempt from these problems was the 4318–4328 cm^{-1} region where strong CH_4 and H_2O absorption bands are absent (see Fig. 1). For the CH_4 absorption bands in the 5996–6145 cm^{-1}, the pressure retrieval yielded accurate results. The CH_4 HITRAN08 database for this range relies on the line list published by Frankenberg et al. (2008) who focused on pressure-broadening effects.

We also inverted 45 spectra from one single observation day at Park Falls to check for air-mass dependent errors. Up to SZA ≈65 degrees, no systematic influence of air-mass was found for CH_4, nor for CO columns. For larger SZA, the discrepancies caused by different averaging kernels increased to the extent to which they masked any potential spectroscopy-related errors.

3.2 CO retrieval accuracy

In contrast to CH_4 and H_2O, the CO absorption maxima are relatively sharp and well separated from each other. Nonetheless, inversion of CO in the SWIR is non-trivial because the CO signature has to be separated from the much stronger background of CH_4 and H_2O absorption. If possible, we would like to retrieve all three species at the same time, using the entire spectral range of 4190–4340 cm^{-1}. This approach worked reasonably well for CH_4.

Figure 6 shows the time-series of retrieved CO (upper panel) and the relative differences of CO columns retrieved at the TROPOMI resolution compared to window 5 at the original resolution (lower panel). The two biases were added

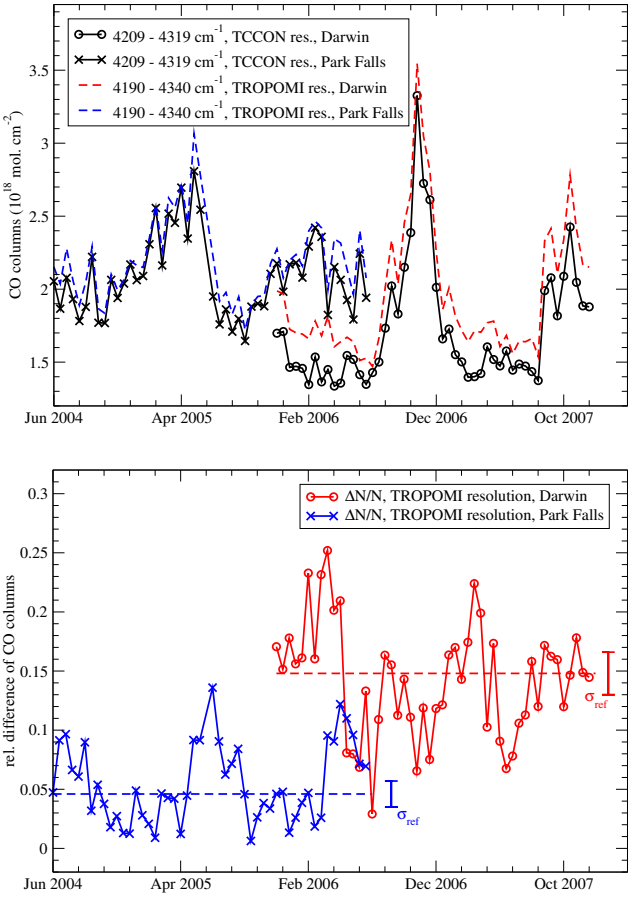

Fig. 6. CO retrieval accuracy at 4190–4340 cm^{-1} for Darwin (circles) and Park Falls (crosses). The upper panel shows the time-series, the lower panel shows the relative differences between columns retrieved at TROPOMI resolution and columns retrieved from window 5 (original high resolution).

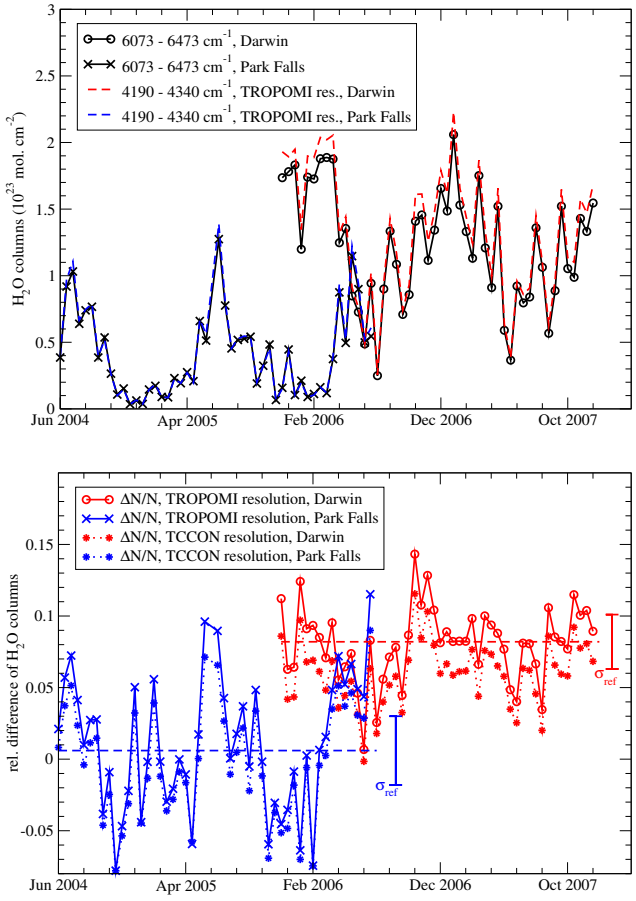

Fig. 7. H_2O retrieval accuracy at 4190–4340 cm^{-1} for Darwin (circles) and Park Falls (crosses). The upper panel shows the time-series, the lower panel shows the relative differences between columns retrieved at 4190–4340 cm^{-1} (for TROPOMI and original high resolution) and columns retrieved from window 4.

as dashed lines in the lower panel. Table 3 lists the corresponding fit diagnostics. The CO retrieval accuracy obviously deteriorated for TROPOMI-like settings. First, the bias b increased from a few to roughly ten percent. Second, the standard deviation of the retrieved CO column error, σ_N, increased by a factor of two to three compared to the reference uncertainty. The increase of bias and standard deviation was more pronounced at Darwin than at Park Falls. An explanation might be that the average H_2O abundance at Darwin was two times higher. We will examine this conjecture in the following. The impact of CH_4 spectroscopic errors on CO retrievals is hard to identify because the atmospheric CH_4 abundance varies little compared to H_2O.

We fitted H_2O and HDO as interfering absorbers while retrieving the CH_4 and CO columns. Figure 7 compares the H_2O columns retrieved from the TROPOMI range to the columns retrieved from window 4 (around 6200 cm^{-1}). The upper panel shows the time-series; the lower panel shows the relative differences to the reference results from window 4

Table 3. Fit diagnostics of the CO column retrievals for the TROPOMI resolution.

	$\langle\chi^2/\nu\rangle$	σ_N	σ_{ref}	b	ξ
Darwin	43	4.8 %	1.8 %	0.148	0.99
Park Falls	32	3.3 %	1.1 %	0.046	0.97

(same format as Fig. 3 for CH_4). Table 4 lists the corresponding fit diagnostics of H_2O, including results from the original (TCCON) and the lower (TROPOMI) resolution. As for CH_4, the H_2O retrieval accuracy did not deteriorate when the input spectrum was degraded to the TROPOMI resolution; σ_N in Table 4 remained almost identical and $\xi > 0.99$ for all data sets. The bias of 6 or 8 % at Darwin was the only obvious difference between the H_2O derived from the TROPOMI range and from window 4. To prove that the CO retrieval errors, in particular at Darwin, were dominated by H_2O interference errors, we needed more evidence.

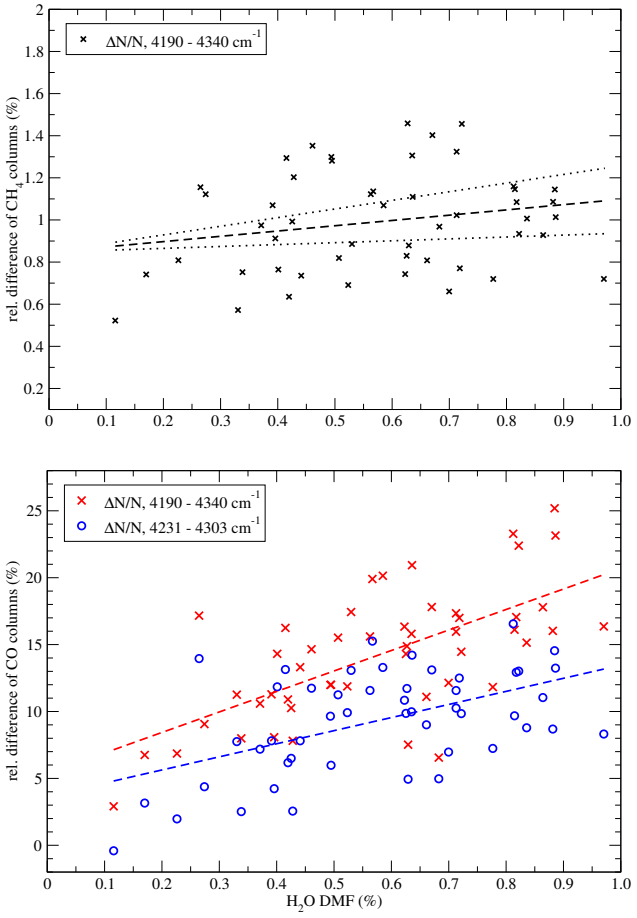

Fig. 8. Correlation of retrieval errors with humidity at Darwin. Deviations of CH_4 (upper panel) and CO columns (lower panel) with respect to the reference values are plotted against H_2O DMF. Red crosses indicate nominal CO retrievals, blue circles show results for an optimised CO sub-window. Dashed lines denote linear fits.

We first replaced our default line list with the HITRAN08 line list to test how sensitively the CO retrieval results reacted to the H_2O spectroscopy. The spectral fit residuals increased by a factor of 2.2 and the H_2O columns were equally biased, whereas the bias of the CO columns changed from 14.8 to 6.7 % at Darwin, and from 4.6 to 1.1 % at Park Falls. On the other hand, the standard deviation of column errors did not decrease significantly.

The CO bias would be of little consequence for the S5P mission if it were constant for all observation sites and atmospheric conditions. A further examination revealed, however, that it strongly depended on the H_2O vapour content. This dependence would introduce undesired seasonal and latitudinal biases for the S5P mission. Figure 8 demonstrates for the Darwin observations the extent to which the CO and CH_4 retrieval errors increased with H_2O abundance. In the lower panel, the CO retrieval errors for the nominal TROPOMI range and for an optimised sub-window (see Sect. 3.3 for further explanation) are plotted against H_2O DMF. The dashed lines show the linear fits, the correlation coefficient calculates to 0.66 for the nominal TROPOMI range and to 0.52 for the sub-window. This correlation did not change when the default H_2O line list was replaced by the HITRAN08 list. Judging from the linear fit, the H_2O-dependence introduced a CO-bias of 15 % between the driest and the most humid day. In contrast to the weak correlation for CH_4, the H_2O interference error on CO is much larger than the reference accuracy.

Table 4. Fit diagnostics of the H_2O column retrievals at the 4190–4340 cm^{-1} range, for the original (TCCON) and for the TROPOMI resolution.

	$\langle\chi^2/\nu\rangle$	σ_N	σ_{ref}	b	ξ
Darwin TROPOMI	43	2.6 %	1.9 %	0.082	0.998
Park Falls TROPOMI	32	4.6 %	2.4 %	0.006	0.999
Darwin TCCON	106	2.2 %	1.9 %	0.061	0.999
Park Falls TCCON	83	4.1 %	2.4 %	−0.004	0.999

In this study, spectroscopic errors are primarily characterised by their impact on retrieved columns. Spectral fit residuals allow us to track down inaccurate absorption lines but do not directly relate to a column inversion error. We correlated the spectral fit residuals to the molecular absorption spectra by calculating Spearman's rank-order correlation coefficient (Press et al., 1986). The correlation with the H_2O absorption spectrum was significant (significance $>10\,\sigma$) for all measurements. The actual correlation strength increased with atmospheric H_2O abundance. For dry atmospheric conditions (H_2O DMF < 0.1 %), the correlation with the CH_4 absorption lines dominated over the H_2O correlation, whereas it became non-significant for wet atmospheric conditions. Figure 5, upper panel, shows a part of the fit residuals for an observation at Darwin with H_2O DMF = 1 %. The cross-sections of H_2O and CH_4, evaluated at $p = 1000$ hPa and $T = 296$ K, are shown as blue and black lines. The residuals peak to the immediate left and right of the absorption maxima of H_2O, whereas the line centres seem to be correct. Inadequate pressure broadening parameters of the strong H_2O absorption lines are an obvious interpretation for this deficiency (see the results on pressure retrievals in Sect. 3.1), but other effects, such as line mixing, probably also contributed to the residuals. There were also fit residuals peaking around CH_4 absorption lines (the lower panel in Fig. 5 shows a Park Falls spectrum for a dry Winter day) but these fit residuals were much more variable in shape and size than their H_2O counterparts.

For the CO retrievals, the 15 % threshold accuracy (Vidot et al., 2012) was met for all 100 examined spectra, but this would be the full error budget for the S5P mission. Moreover, the retrieval errors varied systematically with H_2O and additional errors due to scattering processes of aerosols and clouds are to be expected for a TROPOMI observation

geometry. An improvement of the CO retrieval accuracy is therefore necessary.

3.3 Measures to improve on CO retrieval accuracy

The performance of the CO inversion at TROPOMI resolution is limited by the strong overlapping of the CO with neighbouring CH_4 and H_2O lines, both of which have systematic errors (Fig. 5). Sussmann and Borsdorff (2007) reported that the H_2O interference errors on CO in the 2050–2160 cm^{-1} range were reduced when they retrieved an H_2O profile instead of a scalar value. We experimented with a similar approach for the TROPOMI range, but we did not achieve a notable decrease in CO column error. One reason might be that we relied on an H_2O prior profile already close to the optimum profile.

Another means to reduce interference errors is to restrict the retrieval to a sub-window where the CO absorption lines are more pronounced relative to the CH_4 and H_2O lines. The main drawback of this approach is the loss of information, making the inversion potentially more vulnerable to instrumental effects. For the inversion of back-scattered sunlight, we also have to keep in mind that those parts of the spectrum without CO absorption lines may be needed to retrieve information on scattering particles (Vidot et al., 2012). We defined an overlapping function ω in terms of the spectral sensitivity as

$$\omega = \frac{\left|\frac{\partial I}{\partial N_{H_2O}}\right| + \left|\frac{\partial I}{\partial N_{CH_4}}\right|}{\left|\frac{\partial I}{\partial N_{CO}}\right|}. \quad (4)$$

From Eq. 4 we optimised the CO sub-window by choosing wave number limits k_0, k_1 such that $\sum_{k=k_0}^{k_1} \frac{k_1-k_0}{\omega(k)}$ became maximal. This criterion led to an optimised range of 4231.3–4302.6 cm^{-1} if one contiguous spectral range was to be used. Replacing the nominal TROPOMI range by this sub-window reduced the dependency of the CO retrieval errors with humidity. This is illustrated in Fig. 8, where the retrieval results from the CO sub-window (circles) are compared to the nominal retrieval results (crosses). The bias of the CO columns decreased by 3 to 5 % for both observation sites, and σ_N decreased from 4.8 % to 3.9 % at Darwin and from 3.3 % to 2.7 % at Park Falls.

4 Conclusions

The current H_2O spectroscopy affected, due to interference errors, the CO retrieval accuracy at 4190–4340 cm^{-1} when the TROPOMI resolution was assumed. For wet conditions, the retrieved CO columns deviated by almost 15 % from the result at high spectral resolution. This error correlated with H_2O content in the atmosphere. Because the atmospheric H_2O abundance is highly variable, this would lead to seasonal and latitudinal biases of CO columns for the S5P mission. The CO bias reacted also very sensitively to a different H_2O line list. No shortcomings of the CO spectroscopy itself were detected. The impact of inaccurate CH_4 spectroscopy on CO retrieval errors could not be quantified because of the small variations of atmospheric CH_4. We presented a way to mitigate the impact of interference errors from H_2O and CH_4 by reducing the retrieval window, but a further improvement on H_2O and CH_4 spectroscopy is required for the S5P mission. The loss of information due to a reduced spectral range may pose a problem to the inversion of back-scattered sunlight, for which also scattering properties of the atmosphere need to be retrieved.

For CH_4 column errors, no strong correlation with H_2O abundance was found. The combined H_2O and CH_4 spectroscopy errors caused CH_4 retrieval errors consisting of a constant bias of about 1 % and a standard deviation of about 0.3 %. This is better than the threshold accuracy requirement of 1 % for the S5P mission. Spectroscopy-related errors also manifested themselves in an increase of spectral fit residuals when we compared the TROPOMI spectral range to the 6000 cm^{-1}. This can be caused both by H_2O and by CH_4 spectroscopy. We caution that the intrinsic retrieval accuracy of CH_4 from TCCON spectra is a few tenths of a percent. This means we can only identify spectroscopic deficiencies that result in column errors with the same order of magnitude as the intended accuracy for the S5P mission. For CO, the reference accuracy is an order of magnitude better than the S5P requirement.

Both H_2O and CH_4 showed an incorrect pressure-dependence at 4190–4340 cm^{-1}. This implies that not only the H_2O but also the CH_4 line list is less accurate at the TROPOMI range than around 6000 cm^{-1}. For atmospheric inversion this shortcoming would become important if the surface pressure was to be retrieved from the spectra. Currently, we do not intend such a pressure retrieval for TROPOMI spectra. To improve on the general accuracy of spectroscopic databases, we recommend a similar effort to be directed at the pressure broadening and pressure shift of absorption lines as done by Frankenberg et al. (2008) for CH_4 at 5860–6185 cm^{-1}.

Acknowledgements. This research was funded by the TROPOMI project through NSO. Research leading to these results has received funding from the European Union's Seventh Framework Programme (FP7/2007-2013) under Grant Agreement no. 218793, and by the Dutch User Support Programme under project GO-AO/16. A. Butz is supported by Deutsche Forschungsgemeinschaft (DFG) through the Emmy-Noether programme, grant BU2599/1-1 (RemoteC). US funding for TCCON comes from NASA's Terrestrial Ecology Program, grant number NNX11AG01G, the Orbiting Carbon Observatory Program, the Atmospheric CO_2 Observations from Space (ACOS) Program and the DOE/ARM Program. The Darwin TCCON site was built at Caltech with

funding from the OCO project, and is operated by the University of Wollongong, with travel funds for maintenance and equipment costs funded by the OCO-2 project. We acknowledge funding to support Darwin and Wollongong from the Australian Research Council, Projects LE0668470, DP0879468, DP110103118 and LP0562346. ECMWF ERA Interim analyses are provided through http://data-portal.ecmwf.int/data/d/interimdaily/. TM4 modelled CH_4 and CO concentration fields have been made available through J. F. Meirink, Royal Netherlands Meteorological Institute (KNMI). The CarbonTracker 2010 results have been provided by NOAA ESRL, Boulder, Colorado, USA from the website at http://carbontracker.noaa.gov.

Edited by: J.-L. Attie

References

Bergamaschi, P., Frankenberg, C., Meirink, J. F., Krol, M., Villani, M. G., Houweling, S., Dentener, F., Dlugokencky, E. J., Miller, J. B., Gatti, L. V., Engel, A., and Levin, I.: Inverse modeling of global and regional CH_4 emissions using SCIAMACHY satellite retrievals, J. Geophys. Res., 114, D22301, doi:10.1029/2009JD012287, 2009.

Bovensmann, H., Burrows, J. P., Buchwitz, M., Frerick, J., Noël, S., Rozanov, V. V., Chance, K. V., and Goede, A. P. H.: SCIAMACHY: Mission Objectives and Measurement Modes, J. Atmos. Sci., 56, 127–150, 1999.

Buchwitz, M., Khlystova, I., Bovensmann, H., and Burrows, J. P.: Three years of global carbon monoxide from SCIAMACHY: comparison with MOPITT and first results related to the detection of enhanced CO over cities, Atmos. Chem. Phys., 7, 2399–2411, doi:10.5194/acp-7-2399-2007, 2007.

Butz, A., Guerlet, S., Hasekamp, O., Schepers, D., Galli, A., Aben, I., Frankenberg, C., Hartmann, J.-M., Tran, H., Kuze, A., Keppel-Aleks, G., Toon, G., Wunch, D., Wennberg, P., Deutscher, N. M., Griffith, D., Macatangay, R., Messerschmidt, J., Notholt, J., and Warneke, T.: Toward accurate CO_2 and CH_4 observations from GOSAT, Geophys. Res. Lett., 38, L14812, doi:10.1029/2011GL047888, 2011.

Butz, A., Galli, A., Hasekamp, O., Landgraf, J., Tol, P., and Aben, I.: TROPOMI aboard Precursor Sentinel-5 Precursor: Prospective performance of CH_4 retrievals for aerosol and cirrus loaded atmospheres, Remote Sens. Environ., 120, 267–276, doi:10.1016/j.rse.2011.05.030, 2012.

de Laat, A. T. J., Gloudemans, A. M. S., Schrijver, H., Aben, I., Nagahama, Y., Suzuki, K., Mahieu, E., Jones, N. B., Paton-Walsh, C., Deutscher, N. M., Griffith, D. W. T., De Mazière, M., Mittermeier, R. L., Fast, H., Notholt, J., Palm, M., Hawat, T., Blumenstock, T., Hase, F., Schneider, M., Rinsland, C., Dzhola, A. V., Grechko, E. I., Poberovskii, A. M., Makarova, M. V., Mellqvist, J., Strandberg, A., Sussmann, R., Borsdorff, T., and Rettinger, M.: Validation of five years (2003–2007) of SCIAMACHY CO total column measurements using ground-based spectrometer observations, Atmos. Meas. Tech., 3, 1457–1471, doi:10.5194/amt-3-1457-2010, 2010.

Deeter, M. N., Edwards, D. P., Gille, J. C., and Drummond, J. R.: CO retrievals based on MOPITT near-infrared observations, J. Geophys. Res., 114, D04303, doi:10.1029/2008JD010872, 2009.

Deutscher, N. M., Griffith, D. W. T., Bryant, G. W., Wennberg, P. O., Toon, G. C., Washenfelder, R. A., Keppel-Aleks, G., Wunch, D., Yavin, Y., Allen, N. T., Blavier, J.-F., Jiménez, R., Daube, B. C., Bright, A. V., Matross, D. M., Wofsy, S. C., and Park, S.: Total column CO_2 measurements at Darwin, Australia – site description and calibration against in situ aircraft profiles, Atmos. Meas. Tech., 3, 947–958, doi:10.5194/amt-3-947-2010, 2010.

Frankenberg, C., Meirink, J. F., Bergamaschi, P., Goede, A. P. H., Heimann, M., Körner, S., Platt, U., van Weele, M., and Wagner, T.: Satellite chartography of atmospheric methane from SCIAMACHY on board ENVISAT: Analysis of the years 2003 and 2004, J. Geophys. Res., 111, D07303, doi:10.1029/2005JD006235, 2006.

Frankenberg, C., Warneke, T., Butz, A., Aben, I., Hase, F., Spietz, P., and Brown, L. R.: Pressure broadening in the $2V_3$ band of methane and its implication on atmospheric retrievals, Atmos. Chem. Phys., 8, 5061–5075, doi:10.5194/acp-8-5061-2008, 2008.

Fraser, A., Miller, C. C., Palmer, P. I., Deutscher, N. M., Jones, N. B., and Griffith, D. W. T.: The Australian methane budget: Interpreting surface and train-borne measurements using a chemistry transport model, J. Geophys. Res., 116, D20306, doi:10.1029/2011JD015964, 2011.

Gloudemans, A. M. S., Schrijver, H., Hasekamp, O. P., and Aben, I.: Error analysis for CO and CH_4 total column retrievals from SCIAMACHY 2.3 µm spectra, Atmos. Chem. Phys., 8, 3999–4017, doi:10.5194/acp-8-3999-2008, 2008.

Hasekamp, O. P. and Butz, A.: Efficient calculation of intensity and polarization spectra in vertically inhomogeneous scattering and absorbing atmospheres, J. Geophys. Res., 113, D20309, doi:10.1029/2008JD010379, 2008.

Jenouvrier, A., Daumont, L., Régalia-Jarlot, L., Tyuterev, V. G., Carleer, M., Vandaele, A. C., Mikhailenko, S., and Fally, S.: Fourier transform measurements of water vapor line parameters in the 4200–6600 cm^{-1} region, J. Quant. Spectrosc. Ra., 105, 326–355, 2007.

Kasten, F. and Young, A. T.: Revised optical air mass tabels and c approximation formula, Appl. Optics, 28, 4735–4738, 1989.

Kuze, A., Suto, H., Nakajima, M., and Hamazaki, T.: Thermal and near infrared sensor for carbon observation Fourier-transform spectrometer on the Greenhouse Gases Observing Satellite for greenhouse gases monitoring, Appl. Optics, 48, 6716, doi:10.1364/AO.48.006716, 2009.

Meirink, J. F., Eskes, H. J., and Goede, A. P. H.: Sensitivity analysis of methane emissions derived from SCIAMACHY observations through inverse modelling, Atmos. Chem. Phys., 6, 1275–1292, doi:10.5194/acp-6-1275-2006, 2006.

Morino, I., Uchino, O., Inoue, M., Yoshida, Y., Yokota, T., Wennberg, P. O., Toon, G. C., Wunch, D., Roehl, C. M., Notholt, J., Warneke, T., Messerschmidt, J., Griffith, D. W. T., Deutscher, N. M., Sherlock, V., Connor, B., Robinson, J., Sussmann, R., and Rettinger, M.: Preliminary validation of column-averaged volume mixing ratios of carbon dioxide and methane retrieved from GOSAT short-wavelength infrared spectra, Atmos. Meas. Tech., 4, 1061–1076, doi:10.5194/amt-4-1061-2011, 2011.

Parker, R., Boesch, H., Cogan, A., Fraser, A., Feng, L., Palmer, P. I., Messerschmidt, J., Deutscher, N. M., Griffith, D. W. T., Notholt, J., Wennberg, P. O., and Wunch, D.: Methane observations from the Greenhouse Gases Observing SATellite: Comparison

to ground-based TCCON data and model calculations, Geophys. Res. Lett., 38, 2–7, doi:10.1029/2011GL047871, 2011.

Phillips, P.: A technique for the numerical solution of certain integral equations of the first kind, J. Assoc. Comput. Mach., 9, 84–97, 1962.

Press, W. H., Flannery, B. P., Teukolsky, S. A., and Vetterling, W. T. (Eds.): Numerical Recipes, The Art of Scientific Computing, Cambridge University Press, Cambridge, UK, 1986.

Reuter, M., Bovensmann, H., Buchwitz, M., Burrows, J. P., Connor, B. J., Deutscher, N. M., Griffith, D. W. T., Heymann, J., Keppel-Aleks, G., Messerschmidt, J., Notholt, J., Petri, C., Robinson, J., Schneising, O., Sherlock, V., Velazco, V., Warneke, T., Wennberg, P. O., and Wunch, D.: Retrieval of atmospheric CO_2 with enhanced accuracy and precision from SCIAMACHY: Validation with FTS measurements and comparison with model results, J. Geophys. Res., 116, D04301, doi:10.1029/2010JD015047, 2011.

Rothman, L. S., Gordon, I. E., Barbe, A., Benner, D. C., Bernath, P. F., Birk, M., Boudon, V., Brown, L. R., Campargue, A., Champion, J., Chance, K., Coudert, L. H., Dana, V., Devi, V. M., Fally, S., Flaud, J., Gamache, R. R., Goldman, A., Jacquemart, D., Kleiner, I., Lacome, N., Lafferty, W. J., Mandin, J., Massie, S. T., Mikhailenko, S. N., Miller, C. E., Moazzen-Ahmadi, N., Naumenko, O. V., Nikitin, A. V., Orphal, J., Perevalov, V. I., Perrin, A., Predoi-Cross, A., Rinsland, C. P., Rotger, M., Šimečková, M., Smith, M. A. H., Sung, K., Tashkun, S. A., Tennyson, J., Toth, R. A., Vandaele, A. C., and Vander Auwera, J.: The HITRAN 2008 molecular spectroscopic database, J. Quant. Spectrosc. Ra., 110, 533–572, 2009.

Scheepmaker, R. A., Frankenberg, C., Galli, A., Schrijver, H., Fally, S., Deutscher, N. M., Wunch, D., Warneke, T., and Aben, I.: Improved water vapour spectroscopy in the 4174–4300 cm^{-1} region and its impact on SCIAMACHY's HDO/H_2O measurements, Atmos. Meas. Tech., in preparation, 2012.

Sussmann, R. and Borsdorff, T.: Technical Note: Interference errors in infrared remote sounding of the atmosphere, Atmos. Chem. Phys., 7, 3537–3557, doi:10.5194/acp-7-3537-2007, 2007.

Tikhonov, A.: On the solution of incorrectly stated problems and a method of regularization, Dokl. Akad. Nauk SSSR, 151, 501–504, 1963.

Tran, H., Hartmann, J.-M., Toon, G., Brown, L. R., Frankenberg, C., Warneke, T., Spietz, P., and Hase, F.: The $2\nu3$ band of CH_4 revisited with line mixing: Consequences for spectroscopy and atmospheric retrievals at 1.67 µm, J. Quant. Spectrosc. Ra., 111, 1344–1356, doi:10.1016/j.jqsrt.2010.02.015, 2010.

Veefkind, J. P., Aben, I., McMullan, K., Förster, H., de Vries, J., Otter, G., Claas, J., Eskes, H. J., de Haan, J. F., Kleipool, Q., van Weele, M., Hasekamp, O., Hoogeveen, R., Landgraf, J., Snel, R., Tol, P., Ingmann, P., Voors, R., Kruizinga, B., Vink, R., Visser, H., Levelt, P. F.: TROPOMI on the ESA Sentinel-5 Precursor: A GMES mission for global observations of the atmospheric composition for climate, air quality and ozone layer applications, Remote Sens. Environ., 120, 70–83, doi:10.1016/j.rse.2011.09.027, 2012.

Vidot, J., Landgraf, J., Hasekamp, O. P., Butz, A., Galli, A., Tol, P., and Aben, I.: Carbon monoxide from shortwave infrared reflectance measurements: a new retrieval approach for clear sky and partially cloudy atmospheres, Remote Sens. Environ., 120, 255–266, doi:10.1016/j.rse.2011.09.032, 2012.

Washenfelder, R. A., Toon, G. C., Blavier, J.-F., Yang, Z., Allen, N. T., Wennberg, P. O., Vay, S. A., Matross, D. M., and Daube, B. C.: Carbon dioxide column abundances at the Wisconsin Tall Tower site, J. Geophys. Res., 111, D22305, doi:10.1029/2006JD007154, 2006.

Wunch, D., Toon, G. C., Wennberg, P. O., Wofsy, S. C., Stephens, B. B., Fischer, M. L., Uchino, O., Abshire, J. B., Bernath, P., Biraud, S. C., Blavier, J.-F. L., Boone, C., Bowman, K. P., Browell, E. V., Campos, T., Connor, B. J., Daube, B. C., Deutscher, N. M., Diao, M., Elkins, J. W., Gerbig, C., Gottlieb, E., Griffith, D. W. T., Hurst, D. F., Jiménez, R., Keppel-Aleks, G., Kort, E. A., Macatangay, R., Machida, T., Matsueda, H., Moore, F., Morino, I., Park, S., Robinson, J., Roehl, C. M., Sawa, Y., Sherlock, V., Sweeney, C., Tanaka, T., and Zondlo, M. A.: Calibration of the Total Carbon Column Observing Network using aircraft profile data, Atmos. Meas. Tech., 3, 1351–1362, doi:10.5194/amt-3-1351-2010, 2010.

Wunch, D., Toon, G. C., Blavier, J.-F. L., Washenfelder, R. A., Notholt, J., Connor, B. J., Griffith, D. W. T., Sherlock, V., and Wennberg, P. O.: The Total Carbon Column Observing Network, Philos. T. Roy. Soc. A, 369, 2087–2112, doi:10.1098/rsta.2010.0240, 2011a.

Wunch, D., Wennberg, P. O., Toon, G. C., Connor, B. J., Fisher, B., Osterman, G. B., Frankenberg, C., Mandrake, L., O'Dell, C., Ahonen, P., Biraud, S. C., Castano, R., Cressie, N., Crisp, D., Deutscher, N. M., Eldering, A., Fisher, M. L., Griffith, D. W. T., Gunson, M., Heikkinen, P., Keppel-Aleks, G., Kyrö, E., Lindenmaier, R., Macatangay, R., Mendonca, J., Messerschmidt, J., Miller, C. E., Morino, I., Notholt, J., Oyafuso, F. A., Rettinger, M., Robinson, J., Roehl, C. M., Salawitch, R. J., Sherlock, V., Strong, K., Sussmann, R., Tanaka, T., Thompson, D. R., Uchino, O., Warneke, T., and Wofsy, S. C.: A method for evaluating bias in global measurements of CO2 total columns from space, Atmos. Chem. Phys., 11, 12317–12337, doi:10.5194/acp-11-12317-2011, 2011b.

Yang, Z., Washenfelder, R. A., Keppel-Aleks, G., Krakauer, N. Y., Randerson, J. T., Tans, P. P., Sweeney, C., and Wennberg, P. O.: New constraints on Northern Hemisphere growing season net flux, Geophys. Res. Lett., 34, L12807, doi:10.1029/2007GL029742, 2007.